საქართველოს მეცნიერებათა ეროვნული აკადემიის მოამბე, ტ. 4, №1, 2010
BULLETIN OF THE GEORGIAN NATIONAL ACADEMY OF SCIENCES, vol. 4, no. 1, 2010

Geology

Age of the Madneuli Cu-Au Deposit, Georgia: Evidence from New Nannoplankton Data

Ramaz Migineishvili*, Tamar Gavtadze*

* *A. Janelidze Institute of Geology, Tbilisi*

(Presented by Academy Member M. Topchishvili)

ABSTRACT. A possible model of formation of the Madneuli copper-gold deposit incorporates a sequence of magmatic, tectonic and hydrothermal events occurring contemporaneously with sedimentation of host volcano-sedimentary rocks in a shallow paleosea basin. Identification in these rocks of some biostratigraphic units (CC 20 Zone and CC 22c Subzone) of fossil nannoplanktons enabled the authors to conclude that formation of the Madneuli deposit occurred in Campanian age. Furthermore, dating of the major part of the geological events, proposed by the model, is narrowed down to a short time span of CC 22c nannoplankton Subzone of the Campanian stage. This age is consistent with earlier geochronological findings. *© 2010 Bull. Georg. Natl. Acad. Sci.*

Key words: *VMS-epithermal transition, copper-gold deposit, Campanian, nannoplankton.*

Introduction

The Madneuli copper-gold deposit is located in the southeast part of Georgia, in the Bolnisi ore district. According to tectonic zoning of the Caucasus [1], the Bolnisi ore district is situated in the eastern part of the Artvin-Bolnisi subterrain of the Black Sea-Central Caucasus terrain. The Artvin-Bolnisi subterrain was formed in the framework of an active margin of the Eurasian continent.

Madneuli, as well as a number of copper-gold-barite-polymetallic ore manifestations of the Bolnisi ore district are genetically and spatially tied to the products of subduction-related Late Cretaceous volcansm, although syngenetic ore bodies are known at the Madneuli deposit only. It possesses a number of characteristics that are, in part, typical of Kuroko type volcanogenic massive sulphide (VMS) deposits and partially resemble volcanogenic epithermal copper-gold deposits. It is assigned to a hybrid type of deposits - VMS-epithermal transition [2, 3].

Analysis of lithofacies architecture, as well as of structure of the Madneuli deposit, enabled R.Migineishvili [4] to propose a possible model for its formation. The model implies a sequence of geological processes that presumably occurred in the biography of this deposit.

Stratigraphy of the Upper Cretaceous volcanic-sedimentary rocks of the Bolnisi ore district is based on the investigations of fossil macrofauna [5, 6]. Until very recently, no essential paleontological fossils have been revealed in the host rocks of the Madneuli deposit, so, using lithological correlations they have been assigned to the Upper Turonian-Lower Santonian formations. We have discovered in these rocks a representative association of nannoplankton fossils of the Campanian stage.

This contribution applies to the new paleontological data to create an accurate temporal context for geological processes to be implied by the above-mentioned model.

General description

Geological section of the Madneuli deposit is mainly built of tuff strata of rhyodacitic composition. They form a dome fold structure with gently dipping limbs (Fig.1).

An alternation of coarse- and fine-grained thick-layered tuffs (package 1) occupies the lower stratigraphic level of the section of the deposit and hosts a lenticular silica-rich body (so-called "secondary quartzite"), which is characterized by sharp contact with overlying rocks. In this body, the following zones are identified from top to bottom: quartz-opal, quartz-sericite, and quartz-sericite-chlorite [7].

A breccia-conglomerate apron (package 2) unconformably overlies the above-noted rocks and contains tuff clasts, as well as those generated in the course of erosion of the above-noted silica-rich body. Clasts are angular and rounded. Their sizes vary from 1mm to 1m, but the most common range is 1-10mm. Sometimes its matrix is dominated by fine-grained tuffs, and sometimes by sericite (with minor quartz) aggregate. Within the apron, some tuff interlayers (up to 2-3m in thickness) are also observed. The apron's maximum thickness reaches 45m.

Thin-layered fine-grained tuffs (package 3) follow this section upward. Thickness of this package increases from the top to the peripheries of the Madneuli dome (up to 120 m). It contains second silica-rich (quartz-opal-minor sericite), i.e. "secondary quartzite" body characterized by a stratiform morphology and by sharp conformable contacts with both underlying and overlying rocks. Maximum thickness of this silica-rich body is 80 m, and lateral extent reaches 340 m.

Thus, at the Madneuli deposit there are two silica-rich bodies occupying distinct stratigraphic levels. Presumably, the lower one appeared as a sub-seafloor local hydrothermal alteration, whereas the upper one may have been formed through recrystallization of amorphous cherts accumulated on the seafloor [4, 8]. They also contain minor chalcedony, alunite, kaolinite, pyrophyllite and jarosite. Formation of both silica-rich bodies precedes the ore-forming process, but some minerals (alunite, jarosite, etc.) may have been introduced later as near-ore metasomatites.

Stratigraphically higher thick-layered fine- and medium-grained tuffs (package 4) are exposed. They con-

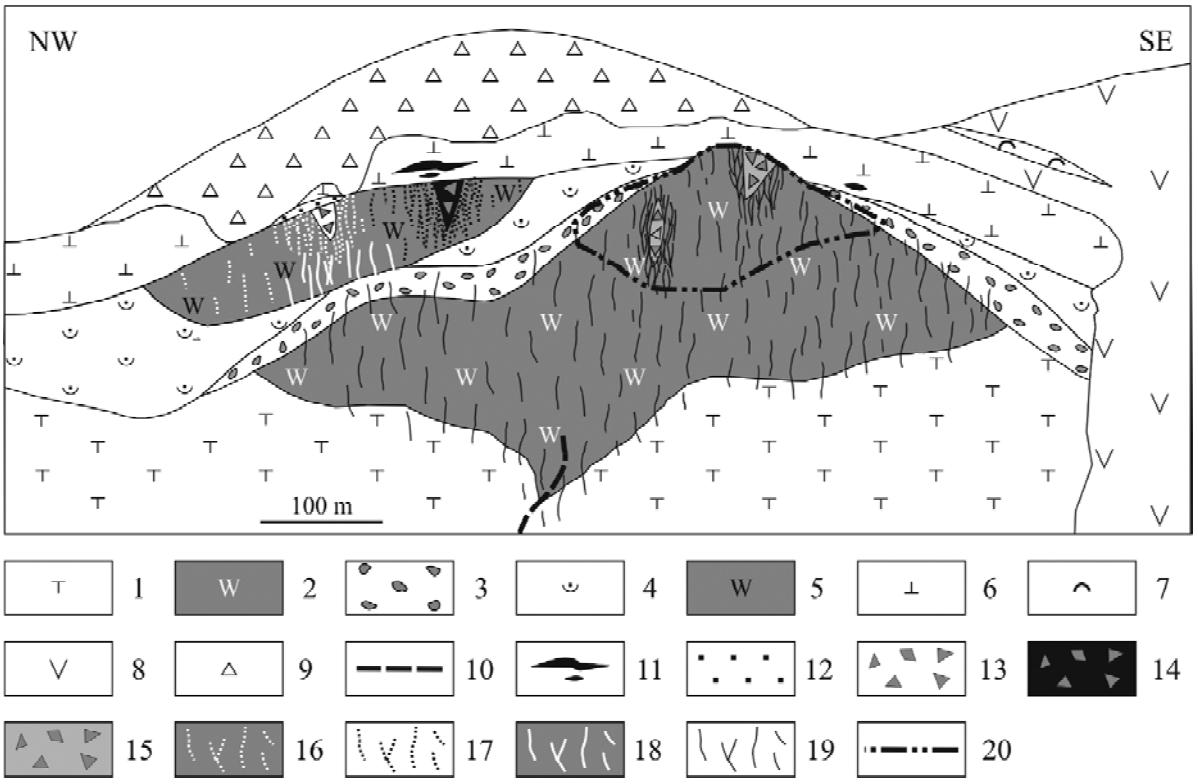

Fig. 1. An idealized geological section through the Madneuli deposit. 1 - Tuff of the first package; 2 - Lower silica-rich body; 3 - Breccia-conglomerate of the second package; 4 - Tuff of the third package; 5 - Upper silica-rich body; 6 - Tuff of the fourth package; 7 - Tuff of the fifth package; 8 - Extrusive body; 9 - Ignimbrite; 10 - Inferred fault; 11-12 - Syngenetic stratiform ores: 11 - Barite-sphalerite-pyrite; 12 - Quartz-barite; 13-15 - Epigenetic breccia ores: 13 - Quartz-barite; 14 - Barite-sphalerite-pyrite; 15 - Quartz-pyrite-chalcopyrite; 16-19 - Epigenetic vein-disseminated ores: 16 - Quartz-barite; 17 - Barite-sphalerite-pyrite; 18 - Chalcopyrite-sphalerite; 19 - Quartz-pyrite-chalcopyrite; 20 - Contour of oxidized ores.

tain rare interlayers of pisolitic tuffs (mainly at the dome top), as well as ore-bearing (sphalerite-pyrite) concretions. The package thickness is about 70 m.

In the south-eastern part of the deposit, there is a rhyodacitic extrusive body. Its effusive "tongue" conformably overlies package 4 and has in its sole a flow breccia. An interlayer of fine-grained tuffs (package 5) is distinguished within this body.

An ignimbrite cover (thickness about 90 m) of rhyodacitic composition caps the deposit. Its sole is characterized by rugged morphology and unconformably overlies the package 4. The ignimbrite is ore-free, but contains scarce xenoliths of silica-rich bodies [9].

At the deposit, there are a number of both sublatitudinal and submeridional (mainly) local faults. Relative movements along them reach several tens of meters. Besides that, here existence of a deep-seated northeast trending fault is inferred [4].

Beneath the Madneuli deposit, 800-900 metres in depth from the present day surface, there is an intrusive body of granodiorite-porphyry and quartz-diorite-porphyry composition.

This deposit contains both epigenetic and syngenetic portions of ore mineralization. The former holds the most part of the Cu-Au reserve and is represented by both vein-disseminated and breccia ores. Breccia ores are characterized by exclusive presence of angular fragments of silica-rich bodies in an ore matrix and occupy the middle and mainly the upper levels of the epigenetic ore zone. They are thought to be formed by fragmentation of host silica-rich bodies due to boiling of hydrothermal solutions [4, 8]. Epigenetic ore mineralisation is mainly confined to silica-rich bodies, which is caused by high fragility and fissuring of these bodies. In the lower silica-rich body, quartz-pyrite-chalcosine-covellite-chalcopyrite ore prevails, whereas the upper one contains a quartz-pyrite-barite-sphalerite-chalcopyrite-galena assemblage. This is a reflection of a mineralogical zoning in a common ore-forming process. This zoning also reflects a strong vertical (from the base to top) gradient in homogenization temperature (in quartz, anhydride, sphalerite, barite, fluorite, gypsum) from chalcopyrite-pyrite-quartz ore (280-345°C), to chalcopyrite-sphalerite-rich ore (255-295°C), to barite-polymetallic ore (160-280°C), and to barite ore (60-180°C) [10]. The upper part of the epigenetic ore zone is oxidized.

Syngenetic ore mineralisation of the deposit is comparatively small in scale and is situated on the top of the epigenetic ore zone. Here, there are syngenetic stratiform ore bodies of the following compositions: barite sand, porous-spongy quartz-barite, banded quartz-barite and massive barite-sphalerite-pyrite.

Besides the main ore-forming minerals, the following less-common minerals are identified at the deposit: brongniardite, tetradymite, aikinite, pavonite, emplectite, bismuthine, enargite, tennantite, freibergite, tetrahedrite, calaverite, krennerite, petzite, dyscrasite, bournonite [11-13]. These minerals occur in close association with chalcopyrite, but paragenetically were introduced later.

At the deposit two generations of gold are established [14]: (i) early fine gold is coeval with the main sulphides, and (ii) later gold formed after the main sulphides. The latter one is presented by native gold in close association with rare-metal group minerals (sulfobismuthites and tellurides), as well as by thread-like (1-2 mm thick) veinlets of bluish-greyish quartz widespread in silica-rich bodies.

Dudauri et al. [15] reported K-Ar isotope dating for the following mineral assemblages of the Madneuli deposit: quartz-sericite - 78±3 Ma; quartz-sericite-chlorite - 78±3 Ma; sericitolite – 85±3 Ma. Based on K-Ar isotope dating, Gugushvili and Omiadze [9] obtained a synvolcanic age of 88 Ma for the intrusive body of granodiorite-porphyry and quartz-diorite-porphyry composition.

Possible model of formation of the Madneuli deposit

Possible model of formation of the Madneuli deposit is divisible into six steps incorporating the following sequence of events [4]:

The first step commenced with deposition of an alternation of coarse- and fine-grained tuffs (package 1) in a shallow sea basin (<200m). The tuffs were sourced from a remote volcano. Simultaneously with the sedimentation, an intrusion of felsic magma beneath the fossil seafloor occurred. A thermal anomaly around it initiated an upflow hydrothermal system focused by the deep-seated northeast trending fault. The front of this system expanded gradually as it neared the seafloor and as a result of a localized hydrothermal replacement of seafloor a funnel-shaped silica-rich body was formed (Fig. 2A).

The first phase of a dome-like local uplift of the seafloor is a major event of **the second step**. The uplift may have been governed by dynamic influence from felsic magma intrusion, emplacement of which was presumably accommodated by the northeast trending deep-seated fault. Due to the uplift, the top of the dome emerged above the sea level and experienced an intensive erosion producing the breccia-conglomerate apron (Fig. 2B). These processes were accompanied by an explosive activity of the remote volcano to form some fine-

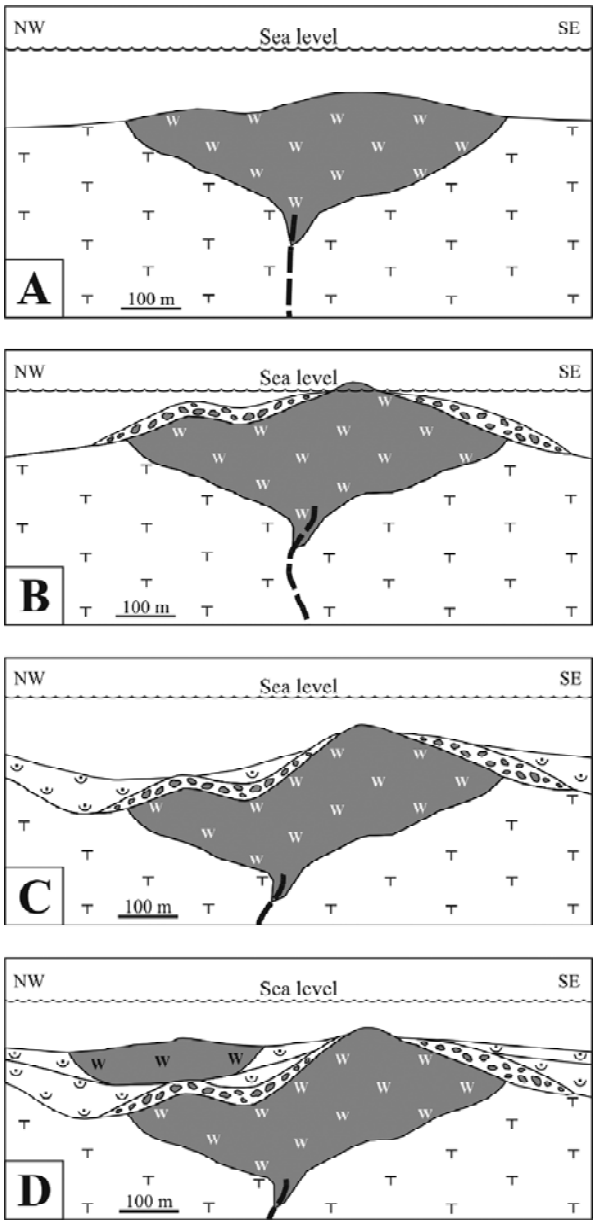

Fig. 2. The first (A), second (B), third (C) and fourth (D) steps of the model. Symbols as for Fig. 1.

grained tuff interlayers within the apron.

The third step implies a subsidence of the territory in question, as well as an intensification of the explosive activity of remote volcano. A possible cause of this subsidence could be a compaction of the intrusive body because of its crystallization, loss of volatile constituents, etc. Due to differentiated movements in the northwestern part of the Madneuli deposit, formation of a local depression is supposed (Fig. 2C). Unconsolidated fine-grained pyroclastic sediments, deposited on the rugged seafloor, moved downward by gravity slumping to form subaqueous pyroclastic flows directed from submerged elevations to comparatively deep parts of the seafloor. The thin-layered fine-grained tuffs (package 3) were deposited from these pyroclastic flows. The thickening of this alternation from the Madneuli dome top to its periphery is a reflection of this redeposition.

During **the fourth step**, sedimentation of the thin-layered fine-grained tuffs (package 3) continued and synchronously with it, functioning of the silica-bearing hydrothermal system recommenced (Fig. 2D). The latter resulted in silicification of some parts of the breccia-conglomerate apron (mostly in the northwestern part of the deposit). Presumably, these hydrotherms vented onto the bottom of the synclinal depression. Synchronously with the venting, the subaqueous pyroclastic flows accumulated new portions of unconsolidated pyroclastic sediments into this depression. Particles of these sediments could serve as nucleation centres for amorphous chert precipitation. As is known from experiments [16], such centres are necessary for silica precipitation. A similar mechanism was suggested for the formation of Kuroko's ferruginous chert layers [17]. The silica-rich upper body of the Madneuli appears to have formed through a later recrystallization of this chert.

The fifth step includes the following three simultaneous processes: (i) sedimentation of thick-layered fine- and medium-grained tuffs (package 4); (ii) reshallowing of ambient seawater; and (iii) ore formation. The reshallowing occurred due to the beginning of a new tendency of seafloor uplift (the second phase of uplift), as well as due to the tuff sedimentation. The dome top presumably elevated up to the sea level (Fig. 3) and in response to small fluctuations in the uplift process, it may have emerged/submerged intermittently. These fluctuations are likely responsible for the formation of the interlayers of pisolitic tuffs within this package. The hydrothermal system of Madneuli remained open to the overlying water column. The major part of the commercial ore mineralization was precipitated below the paleoseafloor, mainly in the silica-rich bodies, whereas a limited discharge of fluids onto the floor led to the formation of the comparatively small-scale stratiform ore bodies occupying the distinct litho-stratigraphic level of the coeval fourth tuff package. The Following two factors may account for such style of ore localization. First, as silica-rich assemblages are the most brittle amongst the host rocks of the deposit [14], they responded to a local tectonic stress field with formation of extensive fracture zones, whereas tuffs deformed in a plastic manner. Second, a destabilization of the physical-chemical equilibrium and a possible boiling of the ore-bearing hydrothermal system may have mostly occurred beneath, rather than above the seafloor. A com-

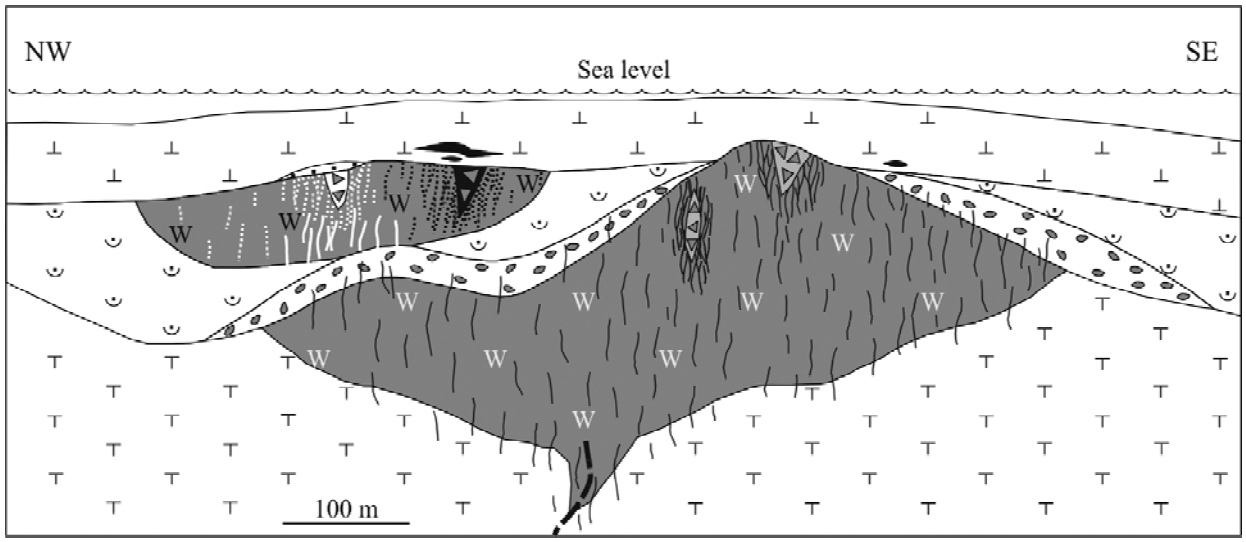

Fig. 3. The fifth step of the model. Symbols as for fig. 1.

paratively low hydrostatic pressure of the overlying shallow water column could not have prevented the fluid boiling. An intensive phase separation process presumably took place within closely fractured zones, and what is important, in immediate proximity to the paleoseafloor. A momentary release of gases may have triggered some impulses of local explosives partially crushing the silica-rich bodies to form the breccia ores.

Fig. 1 demonstrates **the sixth step** of the possible model. In the beginning of it, functioning of the hydrothermal system terminated (or almost terminated). This step represents a peak stage of the second phase of uplift occurring under the influence of the ascending felsic magma. Finally, magma breached the overlying rocks to form the extrusive body. During a short pause in the extrusion process, the fine-grained tuff interlayer of the fifth package was deposited in a submarine setting. Further intensification of the uplift tendency led the whole deposit to a subaerial condition, inducing an intensive erosion and dissection of the paleorelief. In subaerial conditions the ignimbrite cover was formed.

Nannoplankton biostratigraphy

The Cretaceous nannoplankton biozonation, adopted in this study, is that of Sissingh [18] (Fig. 4).

Upper Cretaceous nannoplankton complexes have been revealed in the host rocks of the Madneuli deposit. On the basis of the complexes the following two Campanian biostratigraphic units have been determined in these rocks: (i) Ceratolithoides aculeus Zone (CC 20) and (ii) the Reinhardtites anthophorus Subzone (CC 22c).

Tuffs from the first package contain a complex of nannofossils of the Ceratolithoides aculeus Zone (CC 20): *Ceratolithoides aculeus, Zeugrhabdotus embergeri, Calculites obscurus, Lithastrinus grillii, Prediscosphaera cretacea, P. columnata, C. verbeekii, Lucianorhabdus cayeuxii, L. maleformis, Micula decussate, Quadrum gartneri*. This Zone represents the Upper part of the Lower Campanian and corresponds to a time interval from the first appearance of *Ceratolithoides aculeus* until the first appearance of *Uniplanarius (=Quadrum) sissinghii*.

Coexistence of *Uniplanarius (=Quadrum) trifidus, Reinhardtites anthophorus, R. levis* and *Eiffellithus eximius* in the rocks of the second, third, fourth, and fifth packages defines the Reinhardtites anthophorus Subzone (CC 22c) of the Uniplanarius (=Quadrum) trifidus Zone (CC 22) here. This Subzone represents the lower part of the Upper Campanian and corresponds to a time interval from the first appearance of *R. levis* until the extinction of *R. anthophorus*.

The intermediate Uniplanarius (=Quadrum) sissinghii Zone (CC 21), as well as the lower part of the Uniplanarius (=Quadrum) trifidus Zone (CC 22a+b) has not been identified in the section of the Madneuli deposit. There are two possible explanations for this. First, it might be a result of a sedimentation gap occurring after the formation of the first package. Second, due to an intense hydrothermal alteration, no nannoplankton fossils are preserved in the uppermost part of the first package, so in theory it cannot be excluded that the uppermost part of the first package would represent the biostratigraphic level of the above-noted intermediate Zone/Subzones.

Discussion and conclusions

Since most geological events described in the model occurred contemporaneously with submarine sedimenta-

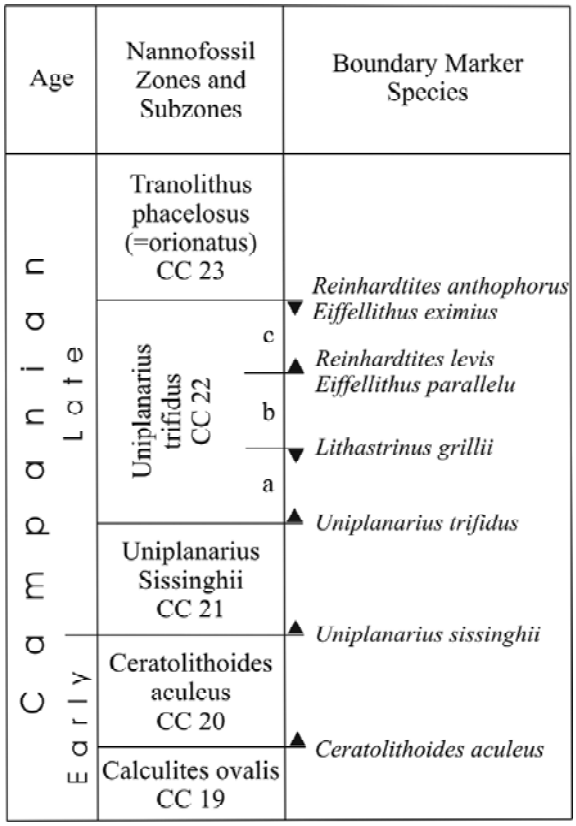

Fig. 4. Campanian nannoplankton biozonation adopted from Sissingh [18].

tion of host rocks, we can date the formation history of the Madneuli deposit, using nannoplankton fossils. Based on this principle we conclude that a major part of the geological processes described in the second, third, fourth, fifth, and sixth (except for the ignimbrite formation) steps of the model took place in a short time frame of CC 22c nannoplankton Subzone of the Campanian age. Formation of the lower silica-rich body (the first step of the model) may have taken place no earlier than CC 20 Zone time, but no later than CC 22c Subzone time of Campanian age.

Campanian age corresponds to a geological time interval that commenced in 83.5±0.7 Ma and was completed in 70.6±0.6 Ma [19]. So, results of K-Ar isotope dating [15] of sericite±quartz±chlorite assemblages of the Madneuli (78±3 Ma and 85±3 Ma) also indicate the Campanian age and are consistent with the results of our investigation. The result of K-Ar isotope dating of the intrusive (88 Ma) [9], which is situated beneath this deposit, presumably corresponds to one of the early episodes of magma emplacement, and formation of the Madneuli deposit may be associated with the later phase(s) of its reactivation that occurred in the Campanian age.

Identification of the specific stratigraphic level, as well as the age of formation of the Madneuli deposit may have a practical implication for exploration in the Bolnisi ore district.

გეოლოგია

მადნეულის სპილენძ-ოქროს საბადოს ფორმირების ასაკი ნანოპლანქტონის ახალი მონაცემების საფუძველზე

რ. მიგინეიშვილი*, თ. ღავთაძე*

* *ა. ჯანელიძის გეოლოგიის ინსტიტუტი, თბილისი*

(წარმოდგენილია აკადემიის წევრის მ. თოფჩიშვილის მიერ)

მადნეულის სპილენძ-ოქროს საბადოს ფორმირების შესაძლო მოდელი მოიცავს მაგმური, ტექტონიკური და ჰიდროთერმული მოვლენების გარკვეულ თანამიმდევრობას, რომლებსაც ადგილი ჰქონდა საბადოს შემცველი ვულკანოგენურ-დანალექი ქანების მარჩხი ზღვის პირობებში სედიმენტაციის თანადროულად. ამ ქანებში განამარხებული ნანოპლანქტონის ბიოსტრატიგრაფიული ერთეულების (CC 20 ზონის და CC 22c ქვეზონის) იდენტიფიცირებამ საშუალება მისცა ავტორებს დაესკვნათ, რომ მადნეულის საბადოს ფორმირება მოხდა

კამპანურ საუკუნეში. უფრო მეტიც, მოდელით ნაგარაუდები გეოლოგიური მოვლენების ძირითადი ნაწილის დათარიღება შემოიფარგლა კამპანური სართულის CC 22c ნანოპლანქტონური ქვეზონის შესაბამისი ხანმოკლე დროის შუალედით. ეს ასაკი შეთავსებადია გეოქრონოლოგიური კვლევების ადრე მიღებულ შედეგებთან.

REFERENCES

1. *E. Gamkrelidze* (1997), Bull. Georg. Acad. Sci., **155,** 3: 422-426.
2. *R. Migineishvili* (2004), Proc. Geol. Inst. Acad. Sci. Georgia. New series, **119**: 755-769 (in Russian).
3. *R. Migineishvili* (2005), Geochemistry, Mineralogy and Petrology, **43**: 128-132.
4. *R. Migineishvili* (2002), Proc. Geol. Inst. Acad. Sci. Georgia. New series, **117**: 472-479.
5. *R. Gambashidze* (1975), Proc. Geol. Inst. Acad. Sci. Georgia. New series, **50**: 69-106 (in Russian).
6. *R. Gambashidze, G. Nadareishvili* (1987), In: G.A.Tvalchrelidze (Ed.) Vulkanizm and formirovanie poleznykh iskopaemykh v podvizhnykh oblastyakh Zemli, Tbilisi: 152-171 (in Russian).
7. *V. Gogishvili* (1980), Sovetskaya Geologiya, **4**: 86-98 (in Russian).
8. *R. Migineishvili* (2000), In: *Gemmell J.B, Pongratz J, (eds)*, Volcanic environments and massive sulfide deposits. CODES Special Publication, **3**: 123-125.
9. *V. Gugushvili, G. Omiadze* (1988), Geologiya rudnykh mestorozhdenii, **30** (2):105-109 (in Russian).
10. *D. Arevadze, V. Gogishvili, V. Yaroshevich* (1983), Geologiya rudnykh mestorozhdenii, **25 (**6): 10-23 (in Russian).
11. *E. Kakhadze* (1963), Doctoral thesis, Tbilisi, 225 pp. (in Russian).
12. *M. Janjgava* (1963), Doctoral thesis, Tbilisi, 238 pp. (in Russian).
13. *Yu. Nazarov* (1966), Osobennosti formirovaniya mestorozhdenii medno-kolchedannoi formatsii Yuzhnoi Gruzii. Moscow, 227 pp. (in Russian).
14. *V. Geleishvili* (1990), Doctoral thesis, Tbilisi, 394 pp. (in Russian).
15. *O. Dudauri, G. Vashakidze, D. Gogoladze* (1990), Soobshch. AN Gruzii, **140** (3): 553-556 (in Russian).
16. *J. Rimstidt, H. Barnes* (1980), Geochim. Cosmochim. Acta, **44**: 1683-1699.
17. *H. Ohmoto* (1996), Ore Geol. Rev., **10**: 135-177.
18. *W. Sissingh* (1977), Géologie en Mijnbouw, **56** (1): 37-65.
19. *J.G. Ogg, G. Ogg, F.M. Gradstein* (2008), The Concise Geologic Time Scale. Cambridge University Press, Cambridge, U.K., 177 pp.

Received September, 2009